This is an *Accepted Manuscript*, which has been through the Royal Society of Chemistry peer review process and has been accepted for publication.

Accepted Manuscripts are published online shortly after acceptance, before technical editing, formatting and proof reading. Using this free service, authors can make their results available to the community, in citable form, before we publish the edited article. We will replace this *Accepted Manuscript* with the edited and formatted *Advance Article* as soon as it is available.

You can find more information about *Accepted Manuscripts* in the **Information for Authors**.

Journal Name

ChemComm

COMMUNICATION

Stepwise modulation of the electron-donating strength of ancillary ligands: understanding the AIE mechanism of cationic iridium(III) complexes

Yong Wu,[a] Hai-Zhu Sun,[a] Hong-Tao Cao,[a] Hai-Bin Li,[a] Guo-Gang Shan,*[a] Yu-Ai Duan,[a] Yun Geng,[a] Zhong-Min Su*[a] and Yi Liao*[b]

Combining the experimental and computational study, AIE mechanism for cationic Ir(III) complexes with triazole-pyridine type ligand has been deciphered for the first time. Larger structural relaxation and weak emissive excited-state intraligand charge transfer (ILCT) characters are responsible for their non-emission in solution, while the non-radiative processes are efficiently restricted in solid-states, enhancing the emission.

Design and construction of efficient luminophores in solid states are of considerable importance to the development of advanced optoelectronic devices.[1] Nevertheless, most of the conventional luminescent materials often suffer from the aggregation-caused quenching (ACQ) effect in the condensed phases,[2] which is harmful for their practical applications. Various approaches have been developed to alleviate the ACQ effect, however, only limited success has been realized. In 2001, an uncommon luminogen system that exhibits more efficient emission in the aggregation state than in solution, termed aggregation-induced emission (AIE), was firstly reported by Tang, which provides a new and feasible strategy to construct highly efficient luminophores.[3] Since then, great efforts have been devoted to the design and synthesis of AIE-active fluorophores.[4] In contrast, the phosphorescent AIE materials have been less exploited,[5] although phosphorescent materials have successfully been reported in extensive application fields due to their promising photophysical properties.[6]

More recently, phosphorescent Ir(III)-based AIE materials have been developed and demonstrated the success in cell imaging and sensing of nitro-explosives.[7] Despite these advances, the design of Ir(III) complexes with AIE characteristics still remains a challenge due to a lack of the clear structure-property relationship. In our research for efficient Ir(III)-based phosphors, we found that such materials could be achieved through introducing either carbazole dendritic group or appropriate functional moieties into the ancillary ligands.[8] However, to the best of our knowledge, the AIE mechanism for cationic Ir(III) complexes is still not clear. It is therefore believed that deciphering the AIE mechanism and understanding the relationship between molecule structure and AIE behavior are valuable for further molecular design. To clarify the reason for the AIE activity, it would be ideal if one can deeply understand the intrinsic photophysical properties for structurally similar AIE and non-AIE Ir(III) complexes.

With this idea in mind, herein we designed and synthesized two cationic Ir(III) complexes **1** and **2** by modulating the electron-donating strength of the ancillary ligand of a reported complex **3** (see scheme 1).[8a] Complexes **2** and **3** exhibit the remarkable AIE feature but **1** does not. To disclose the present AIE mechanism, the detail computational studies on their electronic structures and the intrinsic non-radiative decay processes have been performed. Combining the experimental and theoretical results, it is found that they exhibit a similar energetic profile of the deactivation pathway *via* metal-centered (^{3}MC) state, while the larger structural relaxations as well as weak emissive excited-state characters are responsible for non-emission of **2** and **3** in solutions. The non-radiative pathways such as molecular rotations and vibrations in solid states, however, can be effectively restricted due to the intermolecular packing, resulting in the strong emission.
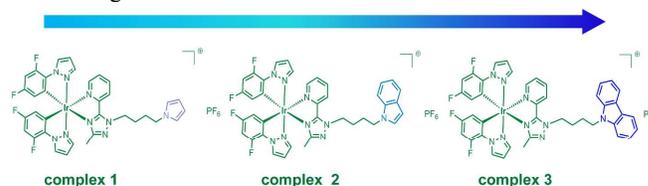
Scheme 1 Chemical structures of cationic Ir(III) complexes **1-3**.

Briefly, two new cationic Ir(III) complexes **1** and **2** were prepared by reacting the organometallated dimer 1-(2,4-difluorophenyl)-1*H*-pyrazole (dfppz) with corresponding ancillary ligands in 1,2-ethandiol, followed by a counter-ion exchange reaction. Detailed procedures and characterization are given in the electronic supplementary information (Fig. S1-Fig. S3, ESI†).

The emission spectra and photoluminescence (PL) quantum efficiency (Φ_{PL}) of complexes **1-3** in different states were measured and the data of Φ_{PL} are summarized in Table S1. As shown in Fig. 1A, **1** exhibits bright green emission at 500 nm with Φ_{PL} of 9.5% in solutions. In sharp contrast, **2** and **3** is almost non-emissive in acetonitrile solution, whose Φ_{PL} is nearly zero and cannot be detected by the integrated sphere system. Clearly,

PL intensities of them reduce with the increase of the electron-donating strength of the ancillary ligand. This indicates that their obviously different emissions in solution will be relative to the substitutions on the ancillary ligand. Although no emissions are observed for complexes **2** and **3** in dilute solution, they show high emissions in solid states with Φ_{PL} of 23.6% and 45.3%, respectively, as shown in Fig. 1B. The above results suggest that complexes **2** and **3** have significant AIE properties, which is further confirmed by their PL spectra in H_2O-CH_3CN mixtures with different water fraction (see Fig. S4, ESI†). Since **2** and **3** are insoluble in water, it is speculated that the aggregates of them will be formed in the mixtures when the water fraction becomes higher. As expected, the amorphous nanoaggregates are formed in the mixtures with water ratio of 90%, which is further supported by the transmission electron microscopy and electron diffraction data (Fig. S5, ESI†). These results confirmed that complexes **2** and **3** are really AIE-active.
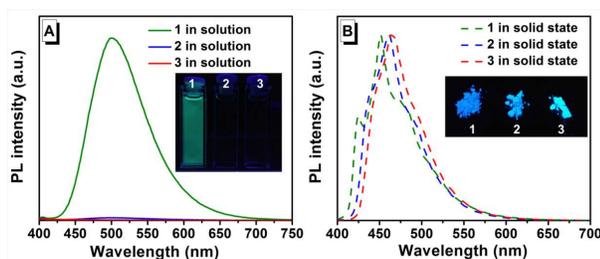

Fig. 1 PL spectra of complexes **1-3** in solutions (A) and solid states (B). Inset: the photogram of **1**, **2** and **3** in solution and solid states taken under 365 nm lamp.

The questions we need to answer now are "why **1** exhibits strong emission in solution, while its analogues **2** and **3** are non-emissive and what is the mechanistic cause for the present AIE effect for complexes **2** and **3**?" To answer these questions, the detail quantum chemical calculations and experimental studies on complexes **1-3** have been carried out, including their potential energy profiles for the thermal deactivation pathway as well as the excited-state characters. For transition metal complexes system such as Ir(III) complex, the photophysical process and excited-state properties are indeed complicated. In general, the strong spin-orbit coupling effect endowed by Ir(III) atom facilitates efficient intersystem crossing from singlet excited-states to triplet manifolds, followed by the internal conversion to the emissive lowest triplet excited state (T_1).[9] In addition to the character of the T_1 state, the roles of non-emissive ^3MC state are very crucial in determining the Φ_{PL} for the transition metal complexes. The thermal population to ^3MC states from T_1 is an effective pathway for non-radiative decay. The relative energies of T_1 and ^3MC states, the energy barrier between T_1 and ^3MC states as well as the positions of $^3MC/S_0$ crossing point are also key parameters for their radiationless decay.[10] As shown in schematic potential energy profiles of the deactivation pathway through ^3MC state (Fig. 2), once the ^3MC state is populated, it can undergo two reaction pathways: (1) returning to the T_1 state *via* a transition state (TS) between T_1 and ^3MC state; (2) encountering the minimum energy crossing point between ^3MC and S_0 potential energy surface.[11] In later case, if T_1-^3MC conversion is energetically accessible and the energy of $^3MC/S_0$ crossing point is close to that of ^3MC state, it would be likely to

undergo fast non-radiative decay back to the ground state. Therefore, the energy differences of ΔE_2 and ΔE_3 play a key role in radiationless pathway. To understand whether the different luminescent behaviors for **1-3** are caused by their different radiationless pathways, the potential energy profiles of the deactivation processes from T_1 *via* the ^3MC state have been studied by employing density functional theory (DFT) method. The geometry optimizations of the complexes in each states and detail calculations are presented in ESI†.
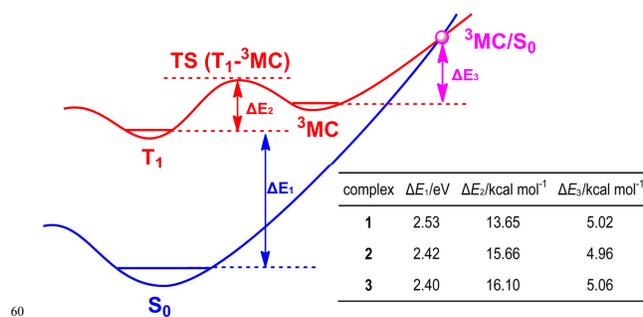

complex	ΔE_1/eV	ΔE_2/kcal mol⁻¹	ΔE_3/kcal mol⁻¹
1	2.53	13.65	5.02
2	2.42	15.66	4.96
3	2.40	16.10	5.06

Fig. 2 Schematic potential energy profiles of the deactivation pathway *via* the ^3MC state. The values computed for adiabatic energy different between S_0 and T_1 (ΔE_1), the activation barrier for the $T_1 \rightarrow {}^3MC$ conversion (ΔE_2) and the energy different between $^3MC/S_0$ and ^3MC (ΔE_3) for complex **1-3** are given.

The calculated ^3MC states for complexes **1-3** are 8.77, 11.38 and 16.10 kcal/mol, respectively, higher in energy than their corresponding T_1 state (Fig. 3). This results indicate that attachment of more strong donating unit on ancillary ligand of cationic Ir(III) complexes can raise the energy of ^3MC state efficiently (Fig. S6, ESI†). The activation barrier for the T_1-^3MC conversion of **1** is about 13.65 kcal/mol, which is also smaller than those of **2** (15.66 kcal/mol) and **3** (16.10 kcal/mol). However, a larger energy barrier from the ^3MC state to T_1 state conversion for **1** is found. In addition, the $^3MC/S_0$ crossing point for **1** is found to be 5.02 kcal/mol above minimum of its ^3MC state, which is comparable to those of **2** (4.96 kcal/mol) and **3** (5.06 kcal/mol) (Fig. S7, ESI†). Thereby, the deactivation process *via* the ^3MC is not the main reason for the non-emission of **2** and **3** in solution. If it does, complex **1** will exhibit much lower Φ_{PL} than **2** and **3** at the same condition, based on the obtained potential energy profiles for complexes **1-3**.

As mentioned above, the character of the T_1 state has an effect on the Φ_{PL}. Time-dependent DFT (TD-DFT) calculations have been performed for **1-3** at their T_1 geometries to provide a deeper understanding of the nature of their emissive states. Selected molecular orbitals for **1-3** are shown in Fig. 3. The LUMOs of complexes **1-3** are almost identical, residing primarily on the pyridine and 1,2,4-triazol groups of ancillary ligands, and not at all on the functional groups, i.e. pyrrole, indole and carbazole moieties. However, significant differences are seen for the occupied molecular orbitals involved in T_1 states. The HOMO-1 for **1** mainly localizes on the cyclometalated ligands and d orbital of iridium atom. On the basis of the TD-DFT calculation and orbital diagrams, the T_1 state of **1** originates from the excitation of HOMO-1→LUMO (91%), with character of mixed metal-to-ligand charge transfer (^3MLCT) and ligand-to-ligand charge transfer (^3LLCT). This is consistent with the board

and featureless emission spectrum of **1** in solution. Nevertheless, the T_1 states of **2** and **3** are both mainly derived from the HOMO → LUMO transition and the HOMOs for them are primarily located on indole and carbazole group, respectively. Consequently, it is suggested that the emissive excited-states of **2** and **3** have a predominant intraligand charge transfer (^{3}ILCT) character, explaining why **2** and **3** show weak emissions in dilute solution.

On the other hand, the remarkable structural relaxation in excited state in principle can induce an efficient radiationless decay pathway. The Huang-Rhys (HR) factors characterize the modification of vibrational quanta when going from one electronic state to another, which has been proved to be a useful parameter to figure out the extent of the geometric distortion.
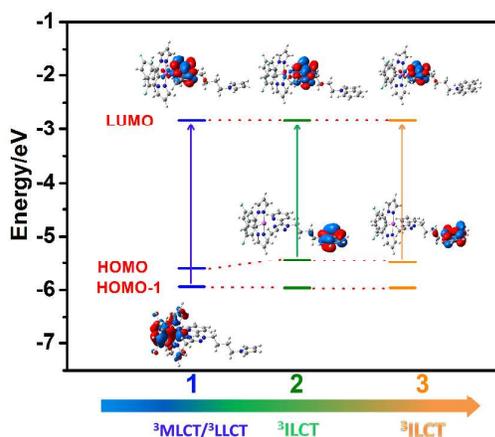

Fig. 3 Selected molecular orbitals involved in the T_1 states of complexes **1-3**. HOMO-1→LUMO for **1**, HOMO→LUMO for **2** and **3**, respectively.

As shown in Fig. S8†, complexes **2** and **3** with relative larger ending-groups possess larger HR factors in either low-frequency regions or high-frequency ones in solution states.[12] The HR factors in general for complexes **2** and **3** are much bigger than that for complex **1**. The significant geometric relaxation in excited-state of **2** and **3** will further increase the radiationless decay pathway and thus no emissions are observed in solution for them. These motions are readily suppressed in aggregate state due to strong intermolecular packing, reducing the non-radiative decay rate, ultimately leading to higher Φ_{PL}. To check the validity of this hypothesis, PL measurements of **2** and **3** doped in PMMA films (preparation method see ESI†) were then carried out. The spectra of corresponding films with different doping concentrations (0.05, 1, 5, 25 and 100 wt%) were measured. As shown in Fig. S9, all doped PMMA films for complexes **2** and **3** exhibit strong emissions even in very low doping concentration of 0.05 wt%. The PL spectra for **2**- and **3**-doped PMMA films show obvious blue-shifts if the concentrations of PMMA are lower than 25 wt%, which may be ascribed in part to the rigidochromic effect. Compared with the emission of **2** and **3** in solution, the molecular rotations and vibrations of both complexes should be restricted to some extent in the PMMA doped or neat films, suppressing the non-radiative decay channels and hence enhanced emission. The low-temperature (77 K) emission of **2** and **3** further prove this conjecture. Upon cooling

the solution of **2** and **3**, the obviously green emissions are observed upon 365 nm UV light irradiation (Fig. S10, ESI†). However, herein there are still no sufficient evidences to testify whether the excited-states of **2** and **3** in solid states are different to those of in solutions. To this objective, we try to carry out the DFT calculations on reported AIE cationic Ir(III) complex with similar parent model based on its crystal structure. The result indicates that the excited-state character has been not changed in crystalline state, which is similar to that in solution (Fig. S11, ESI†). On basis of above experimental and theoretical results, we tentatively attribute the enhanced emission of **2** and **3** in aggregation states to reduction of radiationless decay pathway.

In summary, to deeply understand the AIE mechanism of cationic Ir(III) complexes, three structurally similar Ir(III) complexes **1-3** were designed and synthesized. Among them, **2** and **3** are AIE-active, while such situation is not hold for **1.** We performed detail DFT calculations on the thermal deactivation pathway as well as the electronic structures for AIE Ir(III) systems to decipher their AIE mechanism. The combination experimental and theoretical results suggest that the deactivation processes of them are similar, while the larger structural relaxations as well as weak ILCT emissive excited-states characters are the main reason for their non-emission in solution. The strong emission in solid states is attributed to restriction of non-radiative pathways to some extent. We expect that the results provided here will be helpful guidance for the development of novel cationic Ir(III) complexes with AIE characteristics in future.

Notes and references

^{a}Institute of Functional Material Chemistry, faculty of chemistry, Northeast Normal University, Changchun, 130024 Jilin, People's Republic of China. E-mail: shangg187@nenu.edu.cn; zmsu@nenu.edu.cn
^{b}Department of Chemistry, Capital Normal University, Beijing, People's Republic of China. E-mail: liaoy271@nenu.edu.cn

†Electronic Supplementary Information (ESI) available: [Computational details, synthesis and characterisation of complexes **1-3**, and corresponding photophysical results]. See DOI: 10.1039/c000000x/

1. (*a*) C. W. Tang and S. A. VanSlyke, *Appl. Phys. Lett.*, 1987, **51**, 913; (*b*) S. R. Forrest, M. A. Baldo, D. F. O'Brien, Y. You, A. Shoustikov, S. Sibley and M. E. Thompson, *Nature*, 1998, **395**, 151; (c) Y. Chi and P. T. Chou, *Chem. Soc. Rev.*, 2010, **39**, 638; (*d*) X. Huang, S. Han, W. Huang and X. Liu, *Chem. Soc. Rev.*, 2013, **42**, 173; (*e*) H. Xu, R. Chen, Q. Sun, W. Lai, Q. Su, W. Huang and X. Liu, *Chem. Soc. Rev.*, 2014, 10.1039/c3cs60449g.
2. J. B. Birks, Photophysics of Aromatic Molecules Wiley, London, 1970
3. (*a*) Y. Hong, J. W. J. Lam and B. Z. Tang, *Chem. Soc. Rev.*, 2011, **40**, 5361; (*b*) D. Ding, K. Li, B. Liu and B. Z. Tang, *Acc. Chem. Res.*, 2013, **46**, 2441.
4. (*a*) Z. J. Ning, Z. Chen, Q. Zhang, Y. L. Yan, S. X. Qian, Y. Cao and H. Tian, *Adv. Funct. Mater.*, 2007, **17**, 3799; (*b*) Q. Zeng, Z. Li, Y. Q. Dong, C. A. Di, A. J. Qin, Y. N. Hong, L. Ji, Z. C. Zhu, C. K. W. Jim, G. Yu, Q. Q. Li, Z. A. Li, Y. Q. Liu, J. G. Qin and B. Z. Tang, *Chem. Commun.*, 2007, 70; (*c*) Z. Li, Y. Q. Dong, J. W. Y. Lam, J. Sun, A. Qin, M. Häußler, Y. P. Dong, H. H. Y. Sung, I. D. Williams, H. S. Kwok and B. Z. Tang, *Adv. Funct. Mater.*, 2009, **19**, 905; (*d*)

Y. T. Wu, M. Y. Kuo, Y. T. Chang, C. C. Shin, T. C. Wu, C. C. Tai, T. H. Cheng and W. S. Liu, *Angew. Chem. Int. Ed.*, 2008, **47**, 9891.

5. (*a*) K. Huang, H. Wu, M. Shi, F. Li, T. Yi and C. Huang, *Chem. Commun.*, 2009, 1243; (*b*) Q. Zhao, L. Li, F. Li, M. Yu, Z. Liu, T. Yi and C. Huang, *Chem. Commun.*, 2008, 685; (*c*) C. H. Shin, J. O. Huh, M. H. Lee and Y. Do, *Dalton Trans.*, 2009, 6476; (*d*) S. Liu, H. Sun, Y. Ma, S. Ye, X. Liu, X. Zhou, X. Mou, L. Wang, Q. Zhao and W. Huang, *J. Mater. Chem.*, 2012, **22**, 22167; (*e*) J. Liang, Z. Chen, L. Xu, J. Wang, J. Yin, G.-A. Yu, Z.-N. Chen and S. H. Liu, *J. Mater. Chem. C*, 2014, **2**, 2243.

6. (*a*) K. K.-W. Lo, K. Y. Zhang, S.-K. Leung and M.-C. Tang, *Angew. Chem. Int. Ed.*, 2008, **47**, 2213; (*b*) J. I. Goldsmith, W. R. Hudson, M. S. Lowry, T. H. Anderson and S. Bernhard, *J. Am. Chem. Soc.*, 2005, **127**, 7502; (*c*) M. Mydlak, C. Bizzarri, D. Hartmann, W. Sarfert, G. Schmid and L. De Cola, *Adv. Funct. Mater.*, 2010, **20**, 1812.

7. (*a*) Y. Chen, L. Qiao, B. Yu, G. Li, C. Liu, L. Ji and H. Chao, *Chem. Commun.*, 2013, **49**, 11095; *(b)* K. S. Bejoymohandas, T. M. George, S. Bhattacharya, S. Natarajan and M. L. P. Reddy, *J. Mater. Chem. C*, 2014, **2**, 515; (*c*) X.-G. Hou, Y. Wu, H. Cao, H. Sun, H. Li, G. Shan and Z.-M. Su, *Chem. Commun.*, 2014, **50**, 6031; (*d*) N. Zhao, Y. H. Wu, J. Luo, L. X. Shi and Z. N. Chen, *Analyst*, 2013, **138**, 894.

8. (*a*) G.-G. Shan, H.-B. Li, H.-Z. Sun, D.-X. Zhu, H.-T. Cao and Z.-M. Su, *J. Mater. Chem. C*, 2013, **1**, 1440; (*b*) G. G. Shan, D. X. Zhu, H. B. Li, P. Li, Z. M. Su and Y. Liao, *Dalton Trans.*, 2011, **40**, 2947.

9. (*a*) C. Ulbricht, B. Beyer, C. Friebe, A. Winter and U. S. Schubert, *Adv. Mater.*, 2009, **21**, 4418; (*b*) R. D. Costa, E. Orti, H. J. Bolink, F. Monti, G. Accorsi and N. Armaroli, *Angew. Chem. Int. Ed.*, 2012, **51**, 8178; (c) Y. You and W. Nam, *Chem. Soc. Rev.*, 2012, **41**, 7061.

10. (*a*) F. Alary, M. Boggio-Pasqua, J. L. Heully, C. J. Marsden and P. Vicendo, *Inorg. Chem.*, 2008, **47**, 5259; (*b*) L. Yang, F. Okuda, K. Kobayashi, K. Nozaki, Y. Tanabe, Y. Ishii and M. A. Haga, *Inorg. Chem.*, 2008, **47**, 7154; (c) E. Jakubikova, R. L. Martin and E. R. Batista, *Inorg. Chem.*, 2010, **49**, 2975.

11. (*a*) D. Escudero, E. Heuser, R. J. Meier, M. Schaferling, W. Thiel and E. Holder, *Chem. Eur. J.*, 2013, **19**, 15639; (*b*) W. H. Lam, E. S. Lam and V. W. Yam, *J. Am. Chem. Soc.*, 2013, **135**, 15135.

12. Q. Peng, Y. Yi, Z. Shuai and J. Shao, *J. Am. Chem. Soc.*, 2007, **129**, 9333.